Exploring the influence of operational parameters on the reactivity of elemental iron materials

C. Noubactep[1] (*), T. Licha[1], T.B. Scott[2], M. Fall[3], M. Sauter[1]

[1] Angewandte Geologie, Universität Göttingen, Goldschmidtstrasse 3, D - 37077 Göttingen, Germany

[2] Interface Analysis Centre; University of Bristol, England.

[3] University of Ottawa, Department of Civil Engineering, 161 Louis Pasteur, Ottawa, Ontario, Canada K1N 6N5

(*) corresponding author: cnoubac@gwdg.de; Tel. +49 551 39 3191, Fax. +49 551 399379

Abstract

In an attempt to characterize material intrinsic reactivity, iron dissolution from elemental iron materials (Fe^0) was investigated under various experimental conditions in batch tests. Dissolution experiments were performed in a dilute solution of ethylenediaminetetraacetate (Na_2-EDTA - 2 mM). The dissolution kinetics of eighteen Fe^0 materials were investigated. The effects of individual operational parameters were assessed using selected materials. The effects of available reactive sites [Fe^0 particle size (≤2.0 mm) and metal loading (2-64 g L^{-1})], mixing type (air bubbling, shaking), shaking intensity (0-250 min^{-1}), and Fe^0 pre-treatment (ascorbate, HCl and EDTA washing) were investigated. The data were analysed using the initial dissolution rate (k_{EDTA}). The results show increased iron dissolution with increasing reactive sites (decreasing particle size or increasing metal loading), and increasing mixing speed. Air bubbling and material pre-treatment also lead to increased iron dissolution. The main output of this work is that available results are hardly comparable as they were achieved under very different experimental conditions. A unified experimental procedure for the investigation of processes in Fe^0/H_2O systems is suitable. Alternatively, a parameter (τ_{EDTA}) is introduced which could routinely used to characterize Fe^0 reactivity under given experimental conditions.

Key words: EDTA; Electrochemical reactivity; Operational parameters, Water Remediation; Zerovalent iron.

1. Introduction

Elemental iron (Fe^0) is a well known material for the abiotic removal of organic and inorganic contaminants from groundwater, soils, sediments, and waste streams [1-14]. Fe^0 is widely termed in the literature on permeable reactive barriers as zerovalent iron (ZVI) and is available as Fe^0-based alloys (Fe^0 materials), mostly cast iron and low alloy steel. Reduction through electron transfer from the body of the Fe^0 (direct reduction) is currently considered as the main removal mechanism for the majority of contaminants in Fe^0/H_2O systems [4, 9, 15]. However, for this thermodynamic founded assumption to be realized, the Fe^0 surface has to be accessible to the contaminant species. Alternatively, the surface must be covered by an electron conductive oxide-film (e.g. Fe_3O_4). In all cases, experiments are to be conducted under conditions which closely mimic those found in nature. In particular, mixing of the solution should neither delay nor prevent the formation of an oxide-film in the vicinity of the Fe^0 surface [16, 17]. This aspect of mixing has been mostly overseen since mixing is essentially used as a tool to accelerate contaminant transport to Fe^0 surface [18, 19]. This example illustrates the necessity of exploring and/or revisiting the influence of operational parameters on the processes of iron dissolution which is coupled to contaminant removal.

In the last fifteen years a huge number of studies have been conducted with the aim to understand the impact of operational conditions on the processes of contaminant removal in Fe^0/H_2O systems [2, 15, 18, 20-23]. The investigated experimental conditions included: Fe^0 Characteristics, Fe^0 type, Fe^0 particle size, dissolved oxygen, contaminant concentration, solution chemistry (e.g. pH, dissolved ligands), chemical modification of the original material, mixing type, mixing intensity and material loading. In these studies, the influence of the operational conditions on the removal efficiency for the respective contaminants was reported to be theoretically expected and experimentally verified. For instance, while investigating the effects of mixing intensity (min^{-1}) on nitrate removal by nanoscale Fe^0, Choe et al. [20] found out that for mixing intensities <40 min^{-1} NO_3^- removal is largely a mass

53 transport-limited surface reaction, the reaction taking place at the Fe^0/H_2O interface.
54 However, from open literature on corrosion it is known that under natural conditions (near-
55 neutral pH, slowly flowing groundwater) such an interface does not exist due to the
56 ubiquitous presence of iron oxide that coats the metal surface [24-27] and provides two
57 interfaces; Fe^0/Fe-Oxide and Fe-Oxide/H_2O. The fact that at pH>4.5 an iron surface is always
58 covered with an oxide-film has been recognized in the reactive wall literature [28-31]. For
59 example Chen et al. [29] used a 50 mM ethylenediaminetetraacetate (EDTA) solution to avoid
60 oxide-film formation in their investigations on trichloroethylene degradation by Fe^0. Because
61 the oxide-film is omnipresent at the Fe^0 surface, the interactions of any contaminant in
62 Fe^0/H_2O systems will depend on the nature (composition, conductivity, porosity, thickness) of
63 the formed film and the affinity of the contaminant for the film material. Therefore, it is
64 suitable to characterize Fe^0 reactivity and the effects of operational conditions in systems
65 exempt from in situ generated oxide-films [31]. As a strong iron complexing agent without
66 redox properties EDTA has been used successfully for this purpose [32, 33]. In these previous
67 works [32, 33], a positive correlation between the extend of uranium (VI) removal and the
68 dissolution rates in 2 mM EDTA (k_{EDTA}) was demonstrated for thirteen Fe^0 materials. Recent
69 data on methylene blue discoloration by the same materials corroborated reported results [18].
70 The present study aims to assess the ability of various Fe^0 materials to release Fe (Fe^{II}, Fe^{III}
71 species) into a 2 mM EDTA solution and to establish the response of selected Fe^0 materials to
72 a relative wide range of experimental conditions. The effects of Fe^0 particle size (≤2.0 mm)
73 and metal loading (2-64 g L^{-1}), mixing type (air bubbling, shaking), shaking intensity (0-250
74 min^{-1}), and Fe^0 pre-treatment (ascorbate, HCl and EDTA washing) on Fe dissolution in batch
75 operation mode were investigated and the degree of influence of each examined experimental
76 parameter is discussed.

77 2. Some relevant aspects of the "$Fe^0/EDTA/H_2O$" system

78 Dissolution studies are commonly used as a tool to characterize the reactivity (or stability) of
79 geological materials [34-38]. Using this tool the oxidative dissolution of Fe^0 materials can be
80 investigated at approximately neutral pH in order to simulate pH conditions characteristic of
81 natural groundwaters [39]. Since the solubility of iron in this pH range is very low, EDTA can
82 be used to sustain material dissolution [28, 29, 31]. Table 1 summarises some relevant
83 reactions occurring in a "Fe^0/EDTA/H_2O" system. A very comprehensive review on the
84 chemistry of the "Fe^0/EDTA/H_2O" system is given by Pierce et al. [31].
85 In this system, Fe^0 dissolution is an oxidative process mediated by water (Eq. 1) or dissolved
86 oxygen (Eq. 2). The resultant Fe^{2+} ions can be further oxidized to Fe^{3+} by dissolved O_2 (Eq. 3)
87 or complexed by EDTA, yielding [Fe^{II}(EDTA)] and [Fe^{III}(EDTA)] complexes (Eqs. 4, 5).
88 [Fe^{II}(EDTA)] complexes are highly sensitive to dissolved oxygen, and oxidative
89 transformation to more stable [Fe^{III}(EDTA)] complexes is completed in less than 1 minute
90 [40, 41]. Equations 6 to 8 illustrate the formation of corrosion products and their complexive
91 dissolution by EDTA. Corrosion products are usually mixture of iron oxides (FeOOH, Fe_2O_3,
92 Fe_3O_4); it is expected, that the kinetics of their EDTA dissolution will primarily depend on the
93 crystalline structure of individual oxides [42].
94 The basic approach of this study is to exploit the differences in initial dissolution behaviour of
95 Fe^0 materials in a dilute EDTA solution (2 mM) in order to characterize their intrinsic
96 reactivity [32, 33] and also to investigate the response of the system to changes in some
97 relevant operational parameters. Using a metal loading of 10 g L^{-1} previous works have
98 shown that the dependence of the iron concentration on the elapsed time for the material
99 termed ZVI0 here was a linear function (Eq. 9) for the first 72 hours of the experiment [32,
100 33]. In Eq. 9 $[Fe]_t$ is the total iron concentration at time t as defined by Eq. 10

101 $$[Fe]_t = k_{EDTA} * t + b \quad (9)$$

102 $$[Fe]_t = [Fe^{II}]_t + [Fe^{III}]_t + [Fe^{II}(EDTA)]_t + [Fe^{III}(EDTA)]_t \quad (10)$$

103 The current study was targeted at identifying the time frame for which the linearity of Eq. 9 is
104 assured for the systems "Fe^0 (2 g L^{-1}) / EDTA (2 mM)". For each ZVI material the linear
105 dissolution function obtained from experiment can be used to characterise the individual
106 reactivity, with the linear gradient ('k_{EDTA}' in Eq. 9) representing the rate of iron dissolution
107 (k_{EDTA}) and the intercept ('b' in Eq. 9) representing the iron concentration at t_0 (ideally zero; b
108 = $[Fe]_{to}$), and providing an estimation of the amount of possibly readily soluble atmospheric
109 corrosion products on the material. Ideally, under given experimental conditions, Fe
110 concentration increases continuously with time from 0 mg L^{-1} at the start of the experiment (t_0
111 = 0) to 112 mg L^{-1} (0.002 M) at saturation ($t_{sat} = \tau_{EDTA}$) when a 1:1 complexation of Fe and
112 EDTA occurs. Thus, τ_{EDTA} is an operative parameter which could allow the characterization
113 of the reactivity of each Fe^0 under any experimental conditions [43].
114 An independent process involving Fe^0, EDTA and molecular O_2 was developed by Noradoun
115 and co-wokers [44, 45] and is currently further developed [46-48]. This process uses the
116 "**z**erovalent iron, **E**DTA and **a**ir" system (ZEA system) to generate HO° radicals for
117 contaminant oxidation. In this process, EDTA itself is degraded [46]. Moreover, Gyliene et al.
118 [49] have recently used Fe^0 for aqueous quantitative removal of up to 100 mM EDTA. The
119 removal mechanism included degradation by HO° radicals and co-precipitation with iron
120 corrosion products. The results of Gyliene et al. [49] indicate that under the experimental
121 conditions of this work, EDTA (2 mM) could be removed only by degradation since the Fe^0
122 reactivity characterization is limited to the pre-saturation phase (no precipitation). In total,
123 recent works on the Fe^0/EDTA/H_2O system, clearly demonstrated that EDTA is a concurrent
124 contaminant for in situ generated oxidative species and should be regarded as instable.
125 The present study can be seen as an investigation of the short-term kinetics of iron dissolution
126 in ZEA systems while characterizing the effects of operational parameters on this process.
127 Clearly, a well documented methodology is used to characterize Fe^0 reactivity as influenced
128 by operational parameters. In this method dissolved oxygen is a reactant and not a disturbing

129 factor. Furthermore, since the investigations are limited to the initial phase of iron dissolution
130 (forward dissolution), the possibility that EDTA alters the corrosion process is not likely to be
131 determinant [31]. Theoretically, EDTA should not deplete during this initial reaction phase
132 which is dominated by forward iron dissolution. The well-documented instability of Fe^{III}-
133 EDTA complexes (photodegradation) is the sole concern here [50].

134 ## 3. Material and methods

135 ### 3.1 Solutions

136 Based on previous works [32, 33], a working EDTA solution of 0.002 M (or 2 mM) was used
137 in this study (also see the discussion in the Supporting Information). The working-solution
138 was obtained by one step dilution of a commercial 0.02 M standard from Baker JT® with
139 Milli-Q purified water. A standard iron solution (1000 mg L^{-1}) from Baker JT® was used to
140 calibrate the Spectrophotometer. All other chemicals used were of analytical grade. In
141 preparation for spectrophotometric analysis ascorbic acid was used to reduce Fe^{III}-EDTA in
142 solution to Fe^{II}-EDTA. 1,10 orthophenanthroline (ACROS Organics) was used as reagent for
143 Fe^{II} complexation prior to spectrophotometric determination. Other chemicals used in this
144 study included Na_2-EDTA, $NaHCO_3$, L(+)-ascorbic acid, L-ascorbic acid sodium salt, and
145 sodium citrate. The initial pH of the working EDTA solutions was 5.2 and increased to values
146 above 8.0 as result of iron corrosion.

147 ### 3.2 Fe^0 materials

148 A total of eighteen (18) ZVI materials (ZVI0 through ZVI17) were obtained from various
149 sources, in different forms and grain sizes. The main characteristics of these materials
150 including form, grain size and elemental composition are summarized in Tables SI1 and SI2
151 (Supporting Information). No information about manufacturing processes (e.g. raw material,
152 heat treatment) was available to assist with subsequent data interpretation. It is well reported
153 that the specific surface area (SSA) of iron materials is one of the predominant factors in
154 controlling reactivity and is directly related to grain size [51-53]. The materials investigated in

this study have a variety of different grain sizes (<80 μm to 9000 μm) with resultant differences in specific surface area, although exact values were not available or determined. However, it was not the objective of this study to investigate the impact of the specific surface area on the reactivity of these different materials, but rather to compare the reactivity of the materials in their typical state (and form) in which they might be used for field applications. Apart from samples ZVI0, ZVI7 and ZVI11, all materials were used for experiment in an 'as received' state. Samples ZVI0, ZVI7 and ZVI11 were crushed and sieved, with the grain size fraction between 1 mm and 2 mm selected for reaction.

3.3 Iron dissolution experiments

Three different types of batch experiments were conducted at room temperature (~22 °C) for experimental durations varying from 0.5 to 120 hours. The types of experiment are described in more detail in the following section:

Type 1 open systems: Iron dissolution was initiated by the addition of 0.1 g of each material to 50 mL of a 2 mM EDTA solution (2 g L^{-1} ZVI). Each reaction was run for ≤144 hours (6 days) in triplicate using narrow 70 mL glass beakers to hold the solutions. The reacting samples were left undisturbed on the laboratory bench for the duration of experimental period and were shielded from direct sunlight to minimize Fe^{III}-EDTA photodegradation [50]. These open systems (type 1) were used to characterize: (i) the reactivity of all used Fe^0 (k_{EDTA}, b and τ_{EDTA} values), and (ii) the effects of particle size and mass loading.

Type 2 open systems: Dissolution was initiated by the addition of 0.2 g Fe^0 material in a sealed vessel containing 100 mL of EDTA solution (2 g L^{-1} ZVI). Experiments were conducted for ≤96 hours (4 days) in specially manufactured glass reaction vessels (~125 mL capacity) designed to allow continual mixing of the EDTA solution using a current of humid air supplied by a small aquaristic pump. The setup was designed to homogenize the experimental solutions at atmospheric pressure whilst keeping Fe^0 materials immobile at the bottom of the vessels. Experiments in type 2 open systems were performed to investigate the

impact of mixing art on the process of Fe^0 dissolution. Parallel experiments (non-shaken, ultrasound) were performed in the same vessels to account for possible influence of the reactor geometry.

Closed systems: For each dissolution reaction 0.2 g of the Fe^0 material was added to 100 mL EDTA solution (2 g L^{-1} ZVI) in sealed polypropylene Erlenmeyer flasks (Nalgene®). Each reaction was run for ≤96 hours (4 days) in triplicate. For each experiment the Erlenmeyers were placed on a rotary shaker or in an ultrasonic bath and allowed to react. The shaking intensities used for different samples were 0, 50, 150, 200 and 250 min^{-1}. Closed systems were performed to investigate the effects of mixing intensity.

At various time intervals, 0.100 to 1.000 mL (100 to 1000 μL) of the solution (non filtrated) were withdrawn from the Erlenmeyer flask with a precision micro-pipette and diluted with distilled water to 10 mL (test solution) in 20 mL glass essay tubes in preparation for analysis. After each sampling the equivalent amount of distilled water was added back into the Erlenmeyer in order to maintain a constant volume.

3.4 Analytical method

The aqueous iron concentration was determined with a Varian Cary 50 UV-VIS spectrophotometer, using a wavelength of 510 nm and following the 1,10 orthophenanthroline method [54, 55]. The instrument was calibrated for iron concentration ≤ 10 mg L^{-1}.

The pH value of each sample was measured by combination glass electrodes, that were pre-calibrated with five standards following a multi-point calibration protocol [56] and in accordance with the new IUPAC recommendation [57].

X-ray photoelectron spectroscopy (XPS) was used to identify the atmospheric corrosion products present at the surface of samples ZVI0 and ZVI8. Samples were mounted and analysed under high vacuum (<5 10^{-8} mbar) in a Thermo VG Scientific X-ray photoelectron spectrometer (XPS) equipped with a dual anode X-ray source (Al Kα 1486.6 eV and Mg Kα

206 1253 eV). Al Kα radiation was used at 400W (15 kV) and high resolution scans were
207 acquired using a 30 eV pass energy, 0.1 eV step size and 200 ms dwell times.

208 **4. Results and discussion**

209 **4.1 Expression of experimental results**

210 Given that the initial rate of iron dissolution for each material was expected to follow a linear
211 function ($[Fe]_t = k_{EDTA}*t + b$), regression of the experimental data (Fe concentration versus
212 reaction time) allowed calculation of the linear dissolution function for each individual
213 material. Direct comparison of the calculated rates of iron dissolution (k_{EDTA}) could be used to
214 indicate the more reactive ZVI materials, whilst the calculated intercept ('b') values could be
215 used to indicate the relative amount of pre-existing corrosion products present on the material
216 surfaces. To further characterize Fe^0/EDTA systems, a new parameter is introduced (τ_{EDTA}).
217 Per definition, τ_{EDTA} for a given system is the time require for the iron concentration to reach
218 2 mM (112 mg L^{-1}); that is the time to achieve saturation assuming 1:1 complexation of $Fe^{II,III}$
219 by EDTA. Thus, τ_{EDTA} is the solution of the equation $k_{EDTA}*t + b = 112$. The regression
220 parameters of the experimental data are summarised in two tables (Table 2 and Table 3).

221 **4.2 Qualitative XPS analysis**

222 XPS results from analysis of materials ZVI0 and ZVI8 before experimental reaction clearly
223 indicated that the uppermost surfaces of the two materials were iron oxide. The binding
224 energy of the recorded Fe 2p lines was typical of Fe^{III} in Fe_2O_3 (hematite), although there was
225 some evidence for a minor Fe^{II} oxide (magnetite/wüstite) component. No signal was recorded
226 from the metal, indicating that the materials had a universal oxide coating of at least 10 nm
227 equivalent to the maximum escape depth of photoelectrons from the sample. This result
228 highlights, in agreement with the literature [58-60], the fact that most Fe^0 materials will
229 typical possess a surface oxide coating prior to their use in environmental applications. It has
230 been shown that these coatings are rapidly removed from Fe^0 surfaces upon immersion by an
231 auto-reduction reaction [59, 60]. Removed oxide layers (mostly Fe_2O_3) are subsequently

transformed to magnetite and green rust, which will not inhibit the process of contaminant reduction [59]. However, because reduction is not the fundamental contaminant removal mechanism in Fe^0/H_2O systems [16, 17], it is still interesting to quantify the amount of oxide coatings.

4.3 Effect of operational parameters

Among the tested materials ZVI4 (fillings) was one of the materials exhibiting the largest particle size distribution while exhibiting relative low proportion of fines. ZVI4 was resultantly used in investigations regarding the effects of particle size. Other parameter-testing experiments were conducted with ZVI8 or ZVI0. The preference for ZVI8 is justified by its spherical form, its minor dissolution reactivity (k_{EDTA} and τ_{EDTA} in Table 2) and the fact that the material is rusted and could recover its metallic glaze only after HCl or ETDA washing. While using a less reactive material in experiments where reactivity enhancement is expected (e.g., metal loading, mixing intensity), a large window of opportunity is expected before solution saturation ([Fe] < 112 mg L^{-1}). The available surface area of ZVI8 was estimated using the relation $S = 6/\rho d$ [61], where ρ is the density (7,800 kg m^{-3}) of Fe^0 and d the particle diameter (d = 1.2 mm, Table SI 1).

4.3.1 Effect of Fe^0 type

Eighteen types of Fe^0 materials (Tables SI 1 and SI 2) were evaluated using the EDTA dissolution method described (Type 1 open system). The calculated dissolution rates (k_{EDTA}) are displayed in Table 2 and vary from 1.3 to 111 μg h^{-1}. The large range in reactivity rations recorded for the materials indicates variability in reactivity between the Fe^0 materials. The most reactive material was ZVI 16 (τ_{EDTA} = 2.1 d) displaying a dissolution rate of 111 μg h^{-1}. Scrap iron sample ZVI 7 displayed the lowest dissolution rate (1.3 μg h^{-1}) indicating extremely limited reactivity. The intrinsic difference in the reactivity of various Fe^0 materials may be considered as a significant source for controversial and variable results observed in the literature [18, 19].

The general reactivity trend based on the material form was: powder > fillings > granular. Table 2 shows that some powders (ZVI1, ZVI2, ZVI3) are less reactive than ZVI6 (fillings). This result is mostly justified by the agglomeration of powders under the experimental conditions (non-shaken). Therefore, the EDTA-test may not be appropriate for some powdered materials (d <0.1 mm). The results with ZVI15 (finer grade), ZVI16 (medium grade) and ZVI17 (coarser grade) from Connelly-GPM, Inc. demonstrated that large amounts of fines yield to increased but meaningless b values. Being from the same manufacturer, the three materials have the same chemical composition. Because these materials were used "as received" the observed high b values can be attributed to the proportion of fines.

4.3.2 Effect of metal loading

The effect of the amount of ZVI8 on iron dissolution in 2 mM EDTA was investigated. The material was pre-washed in 50 mL of a 0.25 M HCl for 14 hours to remove surface corrosion products and minimize their subsequent interference. It was found that the rate of iron dissolution increased as the amount of Fe^0 was increased from 2 g to 64 g L^{-1} (or 12 to 410 cm^2 L^{-1}) (Table 3). However, the increase in iron dissolution rates was not linearly proportional to the increase in the amount of Fe^0 reacted (Figure 1). For amounts of material ≤16 g L^{-1} the observed dissolution rates increased at a linear rate with increasing metal loading (R = 0.943) and a normalised iron dissolution rate of 6.2 μg h^{-1} cm^{-2} was estimated. Dissolution rates recorded for metal loads >16 g L^{-1} did not increase at a linear rate. For a more reactive material (e.g. ZVI11) the linearity range would be expected to be lower than for ZVI8 i.e. <16 g L^{-1}. In fact, the more reactive a material the more rapid the kinetics of iron dissolution and thus the shorter the time to solution saturation. 16 g L^{-1} metal load of ZVI8 corresponds to 102 cm^2 L^{-1} available surface.

The surface normalized reaction constant (k_{SA}) is frequently used in evaluating kinetic data from elemental iron reactions and in comparing iron reactivity toward various classes of compounds [51]. The key relationship behind the normalization procedure is linear

284 proportionality between the rate constants and metal loading. There has been controversy over
285 validity of k_{SA} for normalizing the rate constants by metal loading ([21, 62, 63] and references
286 therein]. The results above show that for ZVI8 and under non-shaken conditions linearity is
287 observed only for [ZVI] ≤ 16 g L^{-1} (102 cm^2 L^{-1}). It should be emphasized that mixing will
288 lower this critical mass loading for ZVI8 because of accelerated transport of molecular O_2 to
289 the Fe^0 surface. The large majority of experiments are conducted under mixing conditions and
290 with larger metal loadings. Therefore, the reported significant variations among k_{SA} data (even
291 for a given compound) are difficult to interpret. In the future this comparison should be eased
292 by routinely given τ_{EDTA} for each experimental condition.
293 It is interesting to note that a certain linearity trend of b value as function of mass loading was
294 observed (R = 0.854). This linear dependence of b values from the metal loading validates the
295 enounced signification of that parameter. In this experiment corrosion products resulted from
296 the air oxidation of Fe^0 during the time elapsed between stopping HCl washing and initiating
297 EDTA dissolution. Therefore, the corrosion products didn't have time to precipitate and/or
298 crystallize. As shown above (XPS results), Fe^0 materials are covered with amorphous and
299 crystalline iron oxides with differential dissolution behaviour. For granular materials as ZVI8,
300 it is assumed that the dissolution of iron oxide in EDTA is more favourable than the oxidative
301 dissolution of Fe^0 from the material. This assumption is the support of the significance of b
302 values and could be verified for ZVI0 and ZVI8 used in parallel "as received", 2 mM EDTA-
303 washed, and 250 mM HCl-washed experiments [32]. For materials with large amounts of
304 fines (e.g. powdered materials and ZVI16/ZVI17), however, b values were proven
305 meaningless. Because k_{EDTA} and b values are not independent parameters, erroneous b values
306 have an incidence on the validity of k_{EDTA}. Therefore, the EDTA-test should be limited to
307 coarser material (d > 150 μm). Alternatively, Fe^0 materials can be compared on the basis of
308 extent of leached Fe in column studies (e.g. starting from 1 g of each material). In column

studies saturation is not expected and the differential dissolution of Fe^0 and Fe oxide can be better characterized.

The comparison of a and τ_{EDTA} values (Table 3) for the individual metal loadings shows that reactivity increased 6 fold as the metal loading varies from 2 to 64 g L^{-1}. Considering that essentially higher metal loadings (up to 200 g L^{-1} and more) are used by several researchers another discrepancy source is identified.

As discussed above higher metal loadings are directly related to more iron oxides generation, that are more adsorption sites for all contaminants, including metals and radionuclides. Therefore, in investigating the process of contaminant removal by Fe^0 materials, the less possible metal loading should be used [63]. Considering that ZVI8 contains 92 % Fe, the molar ratio Fe:EDTA varies from 1 to 26 as the mass loading varies from 2 to 64 g L^{-1}. This result shows that, apart from the experiment with 2 g L^{-1}, Fe^0 was available in excess. Characterizing the availability of Fe from the metal structure is a part of this study (see "Effect of Fe^0 type**"**) but using over proportional material excess complicates mechanistic investigations for example. For instance, a lag time (induction time) was reported in the process of contaminant removal by Fe^0 materials [3]. This study shows that the initial iron dissolution is always fast. Therefore, the reported lag time is possibly the time necessary for enough iron oxides to precipitate and adsorb contaminants. Adsorbed contaminants can be further transformed, e.g., reduced by: (i) dissolved Fe^{II}, (ii) oxide-bounded Fe^{II}, (iii) atomic (H) or molecular (H_2) hydrogen.

4.3.3 Effect of Fe^0 particle size

The effect of Fe^0 particle size on the iron dissolution in 2 mM EDTA was investigated using ZVI4. The material was sieved into six particle fractions (Table 3) and an equal mass of each was reacted. The results show increased rates of iron dissolution (increasing k_{EDTA} or decreasing τ_{EDTA}) with decreasing particle size. The evolution of the curve $\tau_{EDTA} = f(d)$ (not shown) suggests that according to particle size, three ranges of reactivity can be distinguished:

335 (i) very reactive (d ≤ 0.2 mm, τ_{EDTA} < 3 d) corresponding to linear increasing of τ_{EDTA} with
336 increasing d; (ii) fairly reactive (0.2 ≤ d(mm) ≤ 0.8, 3 < τ_{EDTA} (d) < 5), corresponding to a
337 plateau in the variation τ_{EDTA} with d; and (iii) less reactive (0.8 ≤ d(mm) ≤ 2.0, τ_{EDTA} > 5 d).
338 This classification suggests that only materials of similar particle sizes should be used in
339 comparative investigations. Based on experimental results it is recommended that for testing
340 micro-scale Fe^0 materials with the EDTA method only particle diameters between 0.1–1.0
341 mm should be tested, ensuring that fines (d ≤ 0.1 mm) are separated by sieving (or washing).
342 The comparison of k_{EDTA} and τ_{EDTA} values for the individual particle sizes shows that
343 dissolution rate significantly decreases as the particle size was varied from ≤ 0.125 to 2.0 mm.
344 This increase of reactivity with decreasing particle size is the rational of using nanoscale Fe^0
345 for environmental remediation [61].

346 **4.3.4 Effect of material pre-treatment**

347 The effect of material pre-treatment was investigated in open systems with a metal loading of
348 5 g L^{-1}. Four different pre-treatment procedures were tested. Pre-treatment consisted of
349 washing 0.5 g of ZVI in 50 mL treatment solution for 14 hours. The treatment solutions
350 included: (i) deionised water (as a reference system), (ii) 0.115 M ascorbate buffer, (iii) 0.02
351 M EDTA, and (iv) 0.25 M HCl. The Fe^0 samples were then rinsed three times with 50 mL
352 deionised water before dissolution testing. The results presented in Table 3 showed that all
353 pre-treatment procedures enhanced the reactivity of ZVI8. The observed iron dissolution rate
354 varied from 560 μg h^{-1} for the reference system to 860 μg h^{-1} for the Fe^0 system washed in
355 0.115 M ascorbate buffer. Calculated τ_{EDTA} values confirmed that the greatest dissolution rate
356 occurred in the ascorbate-treated system. It should be noted that the amount of solid material
357 lost to dissolution during the pre-treatment procedure was not measured in this work.
358 Previously, Matheson and Tratnyek [2] reported a 15 % loss of iron mass during acid pre-
359 treatment (3 hours in 3 % HCl), while Fe^0 washing at neutral pH with ascorbate buffer was

360 found exclusively to dissolve surface corrosion products, leaving a fresh residual Fe^0 surface.
361 Based on the current results it is suggested that ascorbate pre-treatment is a preferable
362 procedure for removing surface corrosion from Fe^0 materials than HCl-washing which has
363 previously been more commonplace.
364 While the effects of pre-treatment generally followed expectation (reactivity enhancement)
365 the relevance of these procedures should be brought into question because Fe^0 materials used
366 in reactive barriers are not commonly pre-treated prior to emplacement [64]. Even if materials
367 were pre-treated before emplacement surface oxides would rapidly form, long before any
368 significant quantity of contaminant inflow [20, 65].

369 **4.3.5 Effect of mixing**

370 In investigating contaminant removal by Fe^0 materials, sample mixing (mostly stirring or
371 shaking) is commonly used as a tool for increasing the rate of reaction. For an inert material
372 as activated carbon, mixing may have little or no effect on material reactivity. However, the
373 thermodynamic instability of metallic iron (Fe^0) in aqueous solution [2, 66] is the primary
374 reason for using elemental iron materials for groundwater remediation.
375 In undisturbed systems in the absence of EDTA, it is generally accepted that decreased Fe^0
376 reactivity observed at pH > 5 is coupled to increased iron precipitation. However, a system
377 which is physically disturbed by mixing will exhibit even greater Fe^0 reactivity because the
378 vigorous hydrodynamic conditions (turbulent flow) increase the rate and amount of iron
379 dissolution/oxidation by: (i) breaking apart and subsequently preventing the aggregation of
380 colloidal iron oxide and oxyhydroxide particles; (ii) continually exposing fresh Fe^0 material
381 through fragment collisions that dislodge and/or remove corrosion products from the material
382 surface, and (iii) causing enhanced oxygen entrainment (diffusion) from the laboratory
383 atmosphere into solution, thereby increasing rates of oxidation. Mixing will also facilitate
384 transport of contaminants and reactive species to the Fe^0 surface although in some cases
385 contaminant desorption may be promoted [67].

386 In this section the effect of mixing on Fe^0 dissolution is presented. Experiments were
387 performed with two materials (ZVI0 and ZVI8) and three mixing types (bubbling,
388 sonification and shaking).

389 **4.3.5.1 Effect of mixing type**

390 Figure 2 summarises the effect of mixing type on the reactivity of ZVI0, the regression
391 parameters and τ_{EDTA} are given in Table 3. The results clearly indicate that all types of sample
392 mixing enhance Fe^0 reactivity. The dissolution rate varied from 33 μg h^{-1} for the non-mixed
393 system to 6154 μg h^{-1} for the ultrasonically mixed system, which displayed the most rapid
394 rate of iron dissolution. This result clearly show that while using different mixing devices and
395 performing the experiments for the same duration (e.g. 4 h) various extents of Fe^0 dissolution
396 was achieved yielding to various amounts of contaminant removal agents (Fe^{II}, H_2, Fe
397 oxides). Characterizing each experimental procedure with τ_{EDTA} will certainly facilitate the
398 discussion of achieved results.

399 **4.3.5.2 Effect of shaking intensity**

400 The effect of shaking intensity was investigated with ZVI8 for four different shaking rates:
401 50, 150, 200 and 250 min^{-1}. The results are summarized in Table 3 and follow theoretical
402 predictions of enhanced dissolution behaviour with increasing mixing intensity. τ_{EDTA} varied
403 from 3.7 days for a mixing intensity of 50 min^{-1} to 0.4 days for 250 min^{-1}. The effect of
404 shaking intensity is presented in more details elsewhere [43]. The results disprove the popular
405 assumption that mixing batch experiments is a tool to limit or eliminate diffusion as dominant
406 transport process of contaminant to the Fe^0 surface.

407 **4.3.5.3 Discussion**

408 Ultrasonic vibration and solution shaking involved the physical movement of both solution
409 and Fe^0 materials. By comparison, solutions mixed by air-bubbling left the Fe^0 material
410 immobile whilst homogenising the overlying solution.

411 The ‘bubbled’ metal-solution system recorded a 40 fold enhancement in reactivity compared
412 to the non-disturbed system. The bubbling maintained a continuously replenished supply of
413 dissolved oxygen to the solution, promoting Fe^0 oxidation and yielding dissolved Fe^{II} and Fe^{III}
414 which then complexed with EDTA. Results indicated a rapid initial dissolution rate for the
415 first 10-15 hours (figure 2) which subsequently tailed off by 80 hours, showing a slight
416 increase again to 120 hours. The observed tail-off in dissolution rate occurred after iron
417 saturation ([Fe] > 112 mg L^{-1}) had been reached and can be attributed to iron oxide nucleation
418 and precipitation. Bubbling supplied the system with unrealistic amounts of dissolved O_2
419 which was unrealistic with regard to subsurface reactive walls. These conditions are
420 encountered in above ground plant for wastewater treatment for which the Fe^0/H_2O system
421 are also used [14].
422 Previous studies have found that sample agitation can disturb, delay or even prevent iron
423 oxide precipitation at the Fe^0 surface [15, 16, 67]. Such mixing may allow contaminant
424 transport to the Fe^0/H_2O interface, an interface which can not exist in nature [24, 63, 65]. On
425 this basis it can be argued that sample mixing and agitation may yield unrealistic results and
426 should therefore be avoided when testing the reactivity of Fe^0 materials for commercial use in
427 reactive barriers [18, 19]. Note that all types of mixing devices can be used for above ground
428 water treatment systems using Fe^0. However, for subsurface applications, mixing should not
429 significantly disturbed the dynamic process of oxide-film formation and transformation.
430 Although the results have shown that Fe^0 reactivity and dissolution may be enhanced by
431 elevated mixing intensities, the mixing process is also known to have an effect on iron oxide
432 precipitation. It is well accepted that contaminants (including EDTA, see ref. [49]) can be
433 entrapped in the matrix of precipitating iron oxides (co-precipitation). Typically, contaminant
434 removal enhanced by mixing is considered to operate on the basis of maintaining a continual
435 supply of freshly exposed Fe^0 surfaces for contaminant uptake. However, it is entirely
436 possible that their co-precipitation with iron oxide may provide a competing removal

mechanism. Even though co-precipitated contaminants can be further reduced by structural Fe^{II} or atomic and molecular hydrogen (H, H_2), the reaction can not quantitatively occur at the Fe^0 surface as commonly reported.

The effect of the mixing intensity on Fe^0 reactivity confirms theoretical predictions but the discussion above questioned the validity of mixing to accelerate contaminant transfer to the Fe^0 surface. It is possible that a critical value exists below which mixing may have limited effect on oxide-film formation (e.g. 40 min^{-1} in [20] or 50 min^{-1} in [43]). However, mixing always increases iron dissolution and the Fe^0 surface is permanently covered with corrosion products. Therefore, it may be advantageous to conduct initial work under stagnant conditions and progressively increase the mixing intensity to discover which mixing speeds can be used without major iron precipitation interference [19]. Clearly, works investigating the same process can only be comparable if conducted under similar τ_{EDTA} conditions.

5. Concluding remarks

The current study aimed at developing a reliable method for comparing and characterising different Fe^0 materials under various experimental conditions. For this purpose an aqueous dissolution method utilizing a dilute 0.002 M EDTA solution was adopted for the experimental work. Results showed that: (i) iron dissolution in non disturbed experiments is a powerful tool for material screening; (ii) mixing type, mixing intensity, particle size and Fe^0 loading enhance the material reactivity to various extents. In particular, material pre-treatment, too rapid mixing speeds or too high Fe^0 dosages may yield reproducible but non realistic results. Since the investigated parameters are not independent from each other it was necessary to introduce a parameter (τ_{EDTA}) which allows a reliable characterization of Fe^0 reactivity under each experimental condition. Therefore, similar to iodine number for activated carbon, τ_{EDTA} is introduced to characterise material reactivity. Ideally, any work with Fe^0 should specify τ_{EDTA} under the experimental conditions. However, despite its practical simplicity, τ_{EDTA} is an extrapolation which accuracy depends on the amount of

463 corrosion products on original materials (b values). Therefore, k_{EDTA} is a better parameter to
464 characterize the reactivity of each Fe^0.
465 Whilst literature on Fe^0 remediation predominantly assumes that contaminant removal mostly
466 occurs though electrochemical reduction at the surface of Fe^0 materials, the results of this
467 study and related works [18, 19, 43, 63] indicated that under environmental conditions
468 contaminant removal may primarily occur in conjunction with the dynamic process of
469 precipitation of corrosion products (non selective process). The first proof for this statement is
470 that Fe^0/H_2O systems have efficiently reduced some contaminants, oxidized some others, and
471 even removed some redox-insensititve contaminants [9, 10, 46]. Therefore, oxidation and
472 reduction should be regarded as subsequent processes in the presence of immersed corroding
473 Fe^0 (statement 1). The concept regarding adsorption and co-precipitation as fundamental
474 contaminant removal mechanisms in Fe^0/H_2O system is based on statement 1. This concept
475 has partly faced with very sceptic views [68, 69]. For example, The authors of [69]
476 complained that this concept "is hardly acceptable since the role of the direct electron transfer
477 in ZVI-mediated reactions is well established and generally accepted among the research
478 community." However, the well-accepted "role of direct electron transfer in ZVI-mediated
479 reactions" was demonstrably a "broad consensus" as recognized by O'Hannesin and Gillham
480 [4]. On the other hand, the authors of [68] were "mystified" by any possible convergence
481 between the mechanism of uranium (U) and an organohalide in Fe^0/H_2O systems because "the
482 topic of U(VI) reduction is clearly remote from that of organohalide reduction". These two
483 examples illustrate the difficulty in revising a well-established but inconsistent concept.
484 Fortunately, electrocoagulation (EC) using iron electrodes (Fe^0 EC) is rigorously an
485 electrochemically accelerated iron corrosion and has proven similar efficiency as passive
486 Fe^0/H_2O systems for the removal of various chemical contaminants and pathogens [70-72].
487 For Fe^0 EC no one has suggested Fe^0 electrodes as reducing agents, because Fe^0 is
488 intentionally corroded to produce "flocs" for contaminant co-precipitation. The similarity

between passive Fe^0/H_2O systems and Fe^0 EC should convince the last sceptics. The scientific community will then concentrate on the further development of the technology.

Interestingly, the scientific community is on schedule to identify the "common underlying mechanisms for reactions" in iron walls that provide a confidence for non-site-specific design. Is this the case, then "site-specific treatability studies may only be required to fine-tune design criteria for the optimal performance of PRBs" [73]. The concept of contaminant adsorption/co-precipitation can be regarded as the first step to this goal. The scientific community should abandon the current approach which merit was to demonstrate the efficiency of Fe^0 for several contaminants (and groups of contaminants). The challenge now is to incorporate future studies within a broad-based understanding of Fe^0 remediation technology. In particular, the removal mechanism of individual contaminants by Fe^0 materials has to be investigated under non disturbed conditions and with realistic metal loadings. The proper use of τ_{EDTA} and k_{EDTA} is a precious guide on this high way.

Acknowledgments

For providing the materials investigated in this study the authors would like to express their gratitude to the branch of the MAZ (Metallaufbereitung Zwickau, Co) in Freiberg (Germany), Gotthart Maier Metallpulver GmbH (Rheinfelden, Germany), Connelly GPM Inc. (USA), Dr. Ralf. Köber from the Institute Earth Science of the University of Kiel and Dr. Vera Biermann from the Federal Institute for Materials Research and Testing (Berlin, Germany). Mechthild Rittmeier and Rüdiger Pfaar are acknowledged for technical support. The manuscript was improved by the insightful comments of anonymous reviewers from Journal of Hazardous Materials. The work was granted by the Deutsche Forschungsgemeinschaft (DFG-No 626/2-1).

Supporting Information Available

Main characteristics and elemental composition of iron materials used in this study;

Discussion on the effect of EDTA initial concentration on iron dissolution.

515 **References**

516 [1] R.W. Gillham, S.F O'Hannesin, Enhanced degradation of halogenated aliphatics by zero-
517 valent iron. Ground Water 32 (1994), 958-967.
518 [2] L.J. Matheson, P.G. Tratnyek, Reductive dehalogenation of chlorinated methanes by iron
519 metal, Environ. Sci. Technol. 28 (1994), 2045-2053.
520 [3] C.G. Schreier, M. Reinhard, Transformation of chlorinated organic compounds by iron
521 and manganese powders in buffered water and in landfill leachate. Chemosphere 29
522 (1994), 1743-1753.
523 [4] S.F. O'Hannesin, R.W. Gillham, Long-term performance of an in situ "iron wall" for
524 remediation of VOCs. Ground Water 36 (1998), 164-170.
525 [5] T. Bigg, S.J. Judd, Zero-valent iron for water treatment. Environ. Technol. 21 (2000), 661-
526 670.
527 [6] D.W. Blowes, C.J. Ptacek, S.G. Benner, W.T. Mcrae Che, T.A. Bennett, R.W. Puls,
528 Treatment of inorganic contaminants using permeable reactive barriers. J. Cont. Hydrol.
529 2000 45, 123-137.
530 [7] M.M. Scherer, S. Richter, R.L. Valentine, P.J.J. Alvarez, Chemistry and microbiology of
531 permeable reactive barriers for in situ groundwater clean up. Rev. Environ. Sci.
532 Technol. 30 (2000), 363–411.
533 [8] J.L. Jambor, M. Raudsepp, K. Mountjoy, Mineralogy of permeable reactive barriers for
534 the attenuation of subsurface contaminants. Can. Miner. 43 (2005), 2117-2140.
535 [9] A.D. Henderson, A.H. Demond, Long-term performance of zero-valent iron permeable
536 reactive barriers: a critical review. Environ. Eng. Sci. 24 (2007), 401-423.
537 [10] A.B. Cundy, L. Hopkinson, R.L.D. Whitby, Use of iron-based technologies in
538 contaminated land and groundwater remediation: A review. Sci. Tot. Environ. 400
539 (2008), 42-51.

[11] R.L. Johnson, R.B. Thoms, R.O'B. Johnson, T. Krug, Field evidence for flow reduction through a zero-valent iron permeable reactive barrier. Ground Water Monit. Remed. 28 (2008), 47-55.

[12] R. Thiruvenkatachari, S. Vigneswaran, R. Naidu, Permeable reactive barrier for groundwater remediation. J. Ind. Eng. Chem. 14 (2008), 145-156.

[13] J. Suk O, S.-W. Jeen, R.W. Gillham, L. Gui, Effects of initial iron corrosion rate on long-term performance of iron permeable reactive barriers: Column experiments and numerical simulation. J. Contam. Hydrol. 103 (2009), 145-156.

[14] T. Pradeep, Anshup, Noble metal nanoparticles for water purification: A critical review. Thin Solid Films (2009), doi:10.1016/j.tsf.2009.03.195 (In Press).

[15] L. Xie, C. Shang, The effects of operational parameters and common anions on the reactivity of zero-valent iron in bromate reduction, Chemosphere 66 (2007), 1652-1659.

[16] C. Noubactep, Processes of contaminant removal in "Fe^0–H_2O" systems revisited: The importance of co-precipitation. Open Environ. J. 1 (2007), 9-13.

[17] C. Noubactep, A critical review on the mechanism of contaminant removal in Fe^0–H_2O systems. Environ. Technol. 29 (2008), 909-920.

[18] C. Noubactep, Characterizing the discoloration of methylene blue in Fe^0/H_2O Systems. J. Hazard. Mater. 166 (2009), 79-87.

[19] C. Noubactep, A.-M.F. Kurth, M. Sauter, Evaluation of the effects of shaking intensity on the process of methylene blue discoloration by metallic iron. J. Hazard. Mater. (In press) doi:10.1016/j.jhazmat.2009.04.046

[20] S. Choe, Y.Y. Chang, K.Y. Hwang, J. Khim, Kinetics of reductive denitrification by nanoscale zero-valent iron, Chemosphere 41 (2000), 1307-1311

[21] H. Song, E.R. Carraway, Reduction of chlorinated methanes by nanosized zero-valent iron: kinetics, pathways and effects of reaction conditions. Environ. Eng. Sci. 23 (2006), 272-284.

566 [22] P. Varanasi, A. Fullana, S. Sidhu, Remediation of PCB contaminated soils using iron
567 nano-particles, Chemosphere 66 (2007), 1031-1038.
568 [23] P. Westerhoff, J. James, Nitrate removal in zero-valent iron packed columns, Water Res.
569 37 (2003), 1818-1830.
570 [24] V. Battaglia, J. Newman, Modeling of a growing oxide film: the iron/iron oxide system.
571 J. Electrochem. Soc. 142 (1995), 1423-1430.
572 [25] E.J. Caule, M. Cohen, The formation of thin films of iron oxide. Can. J. Chem. 33
573 (1955), 288-304.
574 [26] M. Cohen, The formation and properties of passive films on iron. Can. J. Chem. 37
575 (1959), 286-291.
576 [27] M. Stratmann, J. Müller, The mechanism of the oxygen reduction on rust-covered metal
577 substrates. Corros. Sci. 36 (1994), 327-359.
578 [28] A. Abdelouas, W. Lutze, H.E. Nutall, W. Gong, Réduction de l'U(VI) par le fer
579 métallique: application à la dépollution des eaux. C. R. Acad. Sci. Paris Earth Planetary
580 Sci. 328 (1999), 315-319.
581 [29] J.-L. Chen, S.R. Al-Abed, J.A. Ryan, Z. Li, Effects of pH on dechlorination of
582 trichloroethylene by zero-valent iron, J. Hazard. Mater B83 (2001), 243-254.
583 [30] K. Ritter, M.S. Odziemkowski, R.W. Gillham, An in situ study of the role of surface
584 films on granular iron in the permeable iron wall technology. J. Cont. Hydrol. 55 (2002),
585 87-111.
586 [31] E.M. Pierce, D.M. Wellman, A.M. Lodge, E.A. Rodriguez, Experimental determination
587 of the dissolution kinetics of zero-valent iron in the presence of organic complexants.
588 Environ. Chem. 4 (2007), 260-270.
589 [32] C. Noubactep, M. Fall, G. Meinrath, B. Merkel, A simple method to select zero valent
590 iron material for groundwater remediation. paper presented at the Quebec 2004, 57TH

591 Canadian Geotechnical Conference, 5TH Joint CGS/IAH-CNC Conference, Session 1A,
592 (2004) 6-13.
593 [33] C. Noubactep, G. Meinrath, P. Dietrich, M. Sauter, B. Merkel, Testing the suitability of
594 zerovalent iron materials for reactive walls, Environ. Chem. 2 (2005), 71-76.
595 [34] J.S. LaLind, A.T. Stone, Reductive dissolution of goethite by phenolic reductants.
596 Geochim. Cosmochim. Acta 53 (1989), 961-971.
597 [35] J.E. Kostka, K.H. Nealson, Dissolution and reduction of magnetite by bacteria, Environ.
598 Sci. Technol. 29 (1995), 2535-2540.
599 [36] Y. Deng, Effect of pH on the reductive dissolution rates of iron(III) hydroxide by
600 ascorbate, Langmuir 13 (1997), 1835-1839.
601 [37] E.H. Oelkers, General kinetic description of multioxide silicate mineral and glass
602 dissolution, Geochim. Cosmochim. Acta 65 (2001), 3703-3719.
603 [38] N. Schuwirth, T. Hofmann, Comparability of and alternatives to leaching tests for the
604 assessment of the emission of inorganic soil contamination. J Soils Sediments 6 (2005),
605 1-11.
606 [39] L.G.M. Baas-Becking, I.R. Kaplan, D. Moore, Limits of the natural environments in
607 terms of pH and oxidation-reduction potentials. J. Geol. 68 (1960), 243-284.
608 [40] E. Sada, H. Kumazawa, H. Machida, Oxidation kinetics of Fe^{II}-EDTA and Fe^{II}-NTA
609 chelates by dissolved oxygen, Ind. Eng. Chem. Res. 26 (1987), 1468-1472.
610 [41] S. Seibig, R. van Eldik, Kinetics of [Fe^{II}(edta)] oxidation by molecular oxygen revisited.
611 new evidence for a multistep mechanism, Inorg. Chem. 36 (1997), 4115-4120.
612 [42] S. Bonneville, P. Van Cappellen, T. Behrends, Microbial reduction of iron(III)
613 oxyhydroxides: Effects of mineral solubility and availability. Chem. Geol. 212 (2004),
614 255-268.

615 [43] C. Noubactep, Characterizing the effects of shaking intensity on the kinetics of metallic
616 iron dissolution in EDTA. J. Hazard. Mater. (2009) doi:10.1016/j.jhazmat.2009.05.085
617 (In Press).
618 [44] C. Noradoun, M.D. Engelmann, M. McLaughlin, R. Hutcheson, K. Breen, A.
619 Paszczynski, I.F. Cheng, Destruction of chlorinated phenols by dioxygen activation
620 under aqueous room temperature and pressure conditions, Ind. Eng. Chem. Res. 42
621 (2003), 5024-5030.
622 [45] C.E. Noradoun, C.S. Mekmaysy, R.M. Hutcheson, I.F. Cheng, Detoxification of
623 malathion a chemical warfare agent analog using oxygen activation at room temperature
624 and pressure, Green Chem. 7 (2005), 426-430.
625 [46] D.F. Laine, I.F. Cheng, The destruction of organic pollutants under mild reaction
626 conditions: A review. Microchem. J. 85 (2007), 183-193.
627 [47] I. Sanchez, F. Stüber, J. Font, A. Fortuny, A. Fabregat, C. Bengoa, Elimination of phenol
628 and aromatic compounds by zero valent iron and EDTA at low temperature and
629 atmospheric pressure. Chemosphere 68 (2007), 338-344.
630 [48] D.F. Laine, A. Blumenfeld, I.F. Cheng, Mechanistic study of the ZEA organic pollutant
631 degradation system: Evidence for H_2O_2, $HO^{\bullet}$, and the homogeneous cctivation of O_2 by
632 Fe^{II}EDTA. Ind. Eng. Chem. Res. 47 (2008), 6502-6508.
633 [49] O. Gyliene, T. Vengris, A. Stonccius, O. Nivinskien, Decontamination of solutions
634 containing EDTA using metallic iron. J. Hazard. Mater. 159 (2008), 446-451.
635 [50] J. Pietsch, W. Schmidt, F. Sacher, S. Fichtner, H. Brauch, Pesticides and another organic
636 micropollutants in the river Elbe. Fresenius J. Anal. Chem. 353 (1995), 75-82.
637 [51] T.L. Johnson, M.M. Scherer, P.G. Tratnyek, Kinetics of halogenated organic compound
638 degradation by iron metal, Environ. Sci. Technol. 30 (1996), 2634-2640.

639 [52] Y.H. Liou, S.-L. Lo, C.-J. Lin, W.H. Kuan, S.C. Weng, Effects of iron surface
640 pretreatment on kinetics of aqueous nitrate reduction, J. Hazard. Mat. B126 (2005), 189-
641 194.
642 [53] S.M. Ponder, J.G. Darab, T.E. Mallouk, Remediation of Cr(VI) and Pb(II) aqueous
643 solutions using supported, nanoscale zero-valent iron, Environ. Sci. Technol. 34 (2000),
644 2564-2569.
645 [54] W.B. Fortune, M.G. Mellon, Determination of iron with o-phenanthroline: a
646 spectrophotometric study, Ind. Eng. Chem. Anal. Ed. 10 (1938), 60-64.
647 [55] L.G. Saywell, B.B. Cunningham, Determination of iron: colorimetric o-phenanthroline
648 method, Ind. Eng. Chem. Anal. Ed. 9 (1937), 67-69.
649 [56] G. Meinrath, P. Spitzer, Uncertainties in determination of pH. Mikrochem. Acta 135
650 (2000), 155-168.
651 [57] R.P. Buck, S. Rondinini, A.K. Covington, F.G.K. Baucke, C.M.A. Brett, M.F. Camoes,
652 M.J.T. Milton, T. Mussini, R. Naumann, K.W. Pratt, P. Spitzer, G.S. Wilson,
653 Measurement of pH. Definition, standards, and procedures (IUPAC Recommendations
654 2002), Pure Appl. Chem. 74 (2002), 2169-2200.
655 [58] M. Stratmann, K. Hoffmann, In situ Mößbauer spectroscopic study of reactions within
656 rust layers. Corr. Sci. 29 (1989), 1329-1352.
657 [59] K. Ritter, M.S. Odziemkowski, R.W. Gillham, An in situ study of the role of surface
658 films on granular iron in the permeable iron wall technology. J. Contam. Hydrol. 55
659 (2002), 87-111.
660 [60] M.S. Odziemkowski, R.P. Simpraga, Distribution of oxides on iron materials used for
661 remediation of organic groundwater contaminants - Implications for hydrogen evolution
662 reactions. Can. J. Chem./Rev. Can. Chim. 82 (2004), 1495-1506.

663 [61] C. Macé, S. Desrocher, F. Gheorghiu, A. Kane, M. Pupeza, M. Cernik, P. Kvapil, R.
664 Venkatakrishnan, W.-X. Zhang, Nanotechnology and groundwater remediation: A step
665 forward in technology understanding, Remediation 16 (2006), 23-33.
666 [62] C. Noubactep, On the validity of specific rate constants (k_{SA}) in Fe^0/H_2O systems. J.
667 Hazard. Mater. 164 (2009), 835-837.
668 [63] C. Noubactep, An analysis of the evolution of reactive species in Fe^0/H_2O systems, J.
669 Hazard. Mater. doi:10.1016/j.jhazmat.2009.02.143.
670 [64] C. Noubactep, P. Volke, B. Merkel, G. Meinrath, Mitigation of uranium in effluents by
671 zerovalent iron: the role of iron corrosion products. in International Conference on
672 Radioactive Waste Management and Environmental Remediation, 8th. 2001. Bruges,
673 Belgium: **2001** American Society of Mechanical Engineers.
674 [65] T.B. Scott, G.C. Allen, P.J. Heard, M.G. Randell, Reduction of U(VI) to U(IV) on the
675 surface of magnetite. Geochim. Cosmochim. Acta 69 (2005), 5639-5646.
676 [66] E.R. Wilson, The Mechanism of the corrosion of iron and steel in natural waters and the
677 calculation of specific rates of corrosion, Indust. Eng. Chem. 15 (1923), 127-133.
678 [67] N.D. Tomashov, L.P. Vershinina, Kinetics of some electrode processes on a continuously
679 renewed surface of solid metal. Electrochim. Acta 15 (1970), 501-517.
680 [68] M. Elsner, D.M. Cwiertny, A.L. Roberts, B.S. Lollar, Response to Comment on "1,1,2,2-
681 tetrachloroethane reactions with OH-, Cr(II), granular iron, and a copper-iron bimetal:
682 insights from product formation and associated carbon isotope fractionation". Environ.
683 Sci. Technol. 41 (2007), 7949-7950.
684 [69] S.-H. Kang, W. Choi, Response to Comment on "Oxidative degradation of organic
685 compounds using zero-valent iron in the presence of natural organic matter serving as an
686 electron shuttle". Environ. Sci. Technol. 43 (2009), 3966-3967.
687 [70] M.Y.A. Mollah, R. Schennach, J.R. Parga, D.L. Cocke, Electrocoagulation (EC) –
688 science and applications, J. Hazard. Mater. 84 (2001), 29-41.

689 [71] D. Lakshmanan, D.A. Clifford, G. Samanta, Ferrous and ferric ion generation during iron
690 electrocoagulation. Environ. Sci. Technol. 43 (2009), 3853-3859.
691 [72] C.H.A. Moreno, D.L. Cocke, J.A.G. Gomes, P. Morkovsky, J.R. Parga, E. Peterson, C.
692 Garcia, Electrochemical reactions for electrocoagulation using iron electrodes. Ind. Eng.
693 Chem. Res. 48 (2009), 2275-2282.
694 [73] K.L. McGeough, R.M. Kalin, P. Myles, Carbon disulfide removal by zero valent iron.
695 Environ. Sci. Technol. 41 (2007), 4607-4612.
696

696 **Table 1:** Some relevant reactions for the elucidation of the mechanism of ZVI dissolution.

697 oxid. = oxidative, Compl. = complexive.

Process	Reaction equation			Eq.
Iron corrosion	$Fe^0 + 2\ H_2O$	$\Rightarrow$	$Fe^{2+} + H_2 + 2\ HO^-$	(1)
oxid. dissolution	$Fe^0 + ½\ O_2 + H_2O$	$\Leftrightarrow$	$Fe^{2+} + 2\ HO^-$	(2)
Fe^{2+} oxidation	$2\ Fe^{2+} + ½\ O_2 + H_2O$	$\Leftrightarrow$	$2\ Fe^{3+} + 2\ HO^-$	(3)
Fe^{2+} complexation	Fe^{2+} + EDTA	$\Leftrightarrow$	$Fe(EDTA)^{2+}$	(4)
Fe^{3+} complexation	Fe^{3+} + EDTA	$\Leftrightarrow$	$Fe(EDTA)^{3+}$	(5)
$Fe(OH)_3$ formation	$2\ Fe^{2+} + ½\ O_2 + 5\ H_2O$	$\Leftrightarrow$	$2\ Fe(OH)_3 + 4\ H^+$	(6)
$Fe(OH)_3$ aging	$Fe(OH)_3$	$\Leftrightarrow$	FeOOH, (Fe_3O_4, Fe_2O_3)	(7)
Compl. dissolution	FeOOH + EDTA + $3\ H^+$	$\Leftrightarrow$	$Fe(EDTA)^{3+} + 2\ H_2O$	(8)

698

699

700

700 **Table 2**: Corresponding correlation parameters (k_{EDTA}, b, R) and τ_{EDTA} for the fifteen metallic
701 iron materials. As a rule, the more reactive a material is under given conditions the
702 bigger the k_{EDTA} value or the smaller τ_{EDTA}. General conditions: initial pH 5.2, initial
703 EDTA concentration 2 mM, room temperature 23 ± 2 °C, and Fe^0 mass loading 2 g
704 L^{-1}. n is the number of experimental points for which the curve iron vs. time is
705 linear. k_{EDTA} and b-values were calculated in Origin 6.0.
706

Fe^0	**n**	**R**	$\mathbf{k_{EDTA}}$ ($\mu g\ h^{-1}$)	**b** (μg)	$\boldsymbol{\tau_{EDTA}}$ (day)
ZVI7	4	0.992	1.3 ± 0.1	37 ± 8	192.8
ZVI8	5	0.999	18 ± 1	89 ± 12	13.4
ZVI9	5	1.000	24.5 ± 0.3	103 ± 9	9.8
ZVI17	6	0.993	29 ± 2	116 ± 44	7.8
ZVI5	6	0.995	33 ± 2	50 ± 87	7.1
ZVI0	6	0.996	33 ± 1	64 ± 55	7.0
ZVI11	6	0.995	34 ± 2	87 ± 57	6.9
ZVI10	5	0.996	37 ± 3	18 ± 60	6.3
ZVI1	4	0.978	46 ± 6	2280 ± 331	2.9
ZVI4	4	0.987	51 ± 5	241 ± 112	4.3
ZVI2	4	0.974	53 ± 6	2015 ± 351	2.8
ZVI3	4	0.980	57 ± 5	1758 ± 281	2.8
ZVI6	4	0.994	57 ± 6	382 ± 208	4.2
ZVI12	4	0.980	70 ± 15	1679 ± 443	2.5
ZVI14	4	0.995	71 ± 9	644 ± 275	2.6
ZVI13	4	0.995	74 ± 6	968 ± 243	2.7
ZVI15	3	0.993	92 ± 11	642 ± 444	2.2
ZVI16	3	0.996	111 ± 10	65 ± 353	2.1

707
708

Table 3: Corresponding correlation parameters (k_{EDTA}, b, R) and τ_{EDTA} of iron dissolution under various operational conditions. As a rule, the more reactive a material is under given conditions the bigger the k_{EDTA} or the smaller τ_{EDTA}. General conditions: initial pH 5.2, initial EDTA concentration 2 mM, room temperature 23 ± 2 °C, and Fe^0 mass loading 2 g L^{-1}. For the investigation of the effects of material pre-treatment a mass loading of 5 g L^{-1} was used. For each test item the used material is mentioned. n is the number of experimental points for which the curve iron vs. time is linear. k_{EDTA} and b-values were calculated in Origin 6.0. For orientation, n = 7 corresponds to an experimental duration of 5 days in non-disturbed experiments (effects of metal loading and particle size).

Test items	Parameter	n	R	k_{EDTA} μg h^{-1}	b (μg)	τ_{EDTA} (d)
Metal loading	2 g L^{-1}	7	0.993	15 ± 1	46 ± 10	22.7
	4 g L^{-1}	7	0.997	21 ± 1	79 ± 19	11.0
ZVI8	8 g L^{-1}	7	0.997	33 ± 2	56 ± 41	10.2
	16 g L^{-1}	7	0.989	38 ± 3	180 ± 162	5.9
	32 g L^{-1}	7	0.984	75 ± 8	202 ± 107	4.6
	64 g L^{-1}	7	0.978	83 ± 9	223 ± 198	4.0
Fe^0 particle size	0.0-0.125	5	0.986	94 ± 9	1914 ± 222	1.6
	0.125-0.200	5	0.990	77 ± 6	318 ± 135	2.9
ZVI4	0.2-0.315	5	0.993	68 ± 5	78 ± 47	3.4
	0.315-0.500	5	0.983	61 ± 6	138 ± 128	3.7
	0.500-1.00	7	0.985	48 ± 4	138 ± 87	4.7
	1.00-2.00	7	0.996	27 ± 1	33 ± 14	8.7
Fe^0 pre-treatment	none	9	0.988	559 ± 33	609 ± 178	0.79
	H_2O	9	0.983	605 ± 42	722 ± 227	0.72
ZVI8	ascorbate	8	0.992	863 ± 44	594 ± 178	0.51
	EDTA	9	0.993	626 ± 28	366 ± 148	0.72
	HCl	9	0.996	611 ± 20	363 ± 105	0.74
Mixing type	none	10	0.996	33.1 ± 1.1	177 ± 2	13.9
	sonification	4	0.989	6154 ± 637	1926 ± 862	0.1
ZVI0	bubbling	9	0.995	1237 ± 48	340 ± 58	0.4
	shaking	7	0.997	218 ± 19	1096 ± 426	1.9
Mixing intensity	50 min^{-1}	7	0.988	52 ± 4	71 ± 26	3.7
	150 min^{-1}	7	0.995	192 ± 9	264 ± 77	1.9
ZVI8	200 min^{-1}	5	0.990	898 ± 72	758 ± 204	0.5
	250 min^{-1}	4	0.995	1070 ± 79	415 ± 182	0.4

719 **Figure 1**

720

721

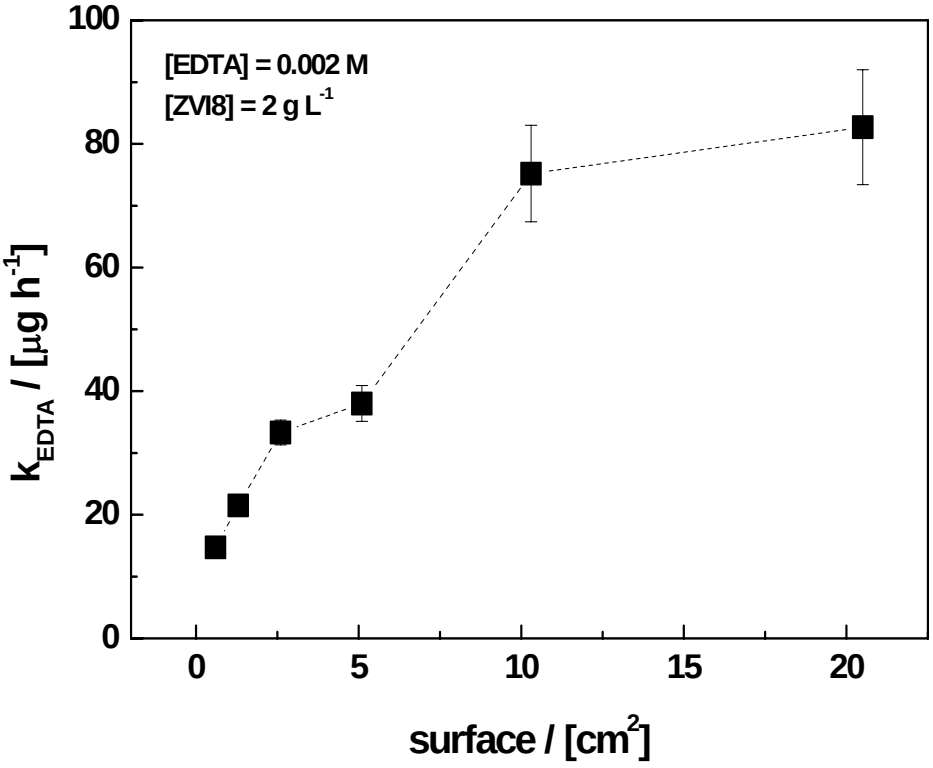

722

723

723 **Figure 2**

724

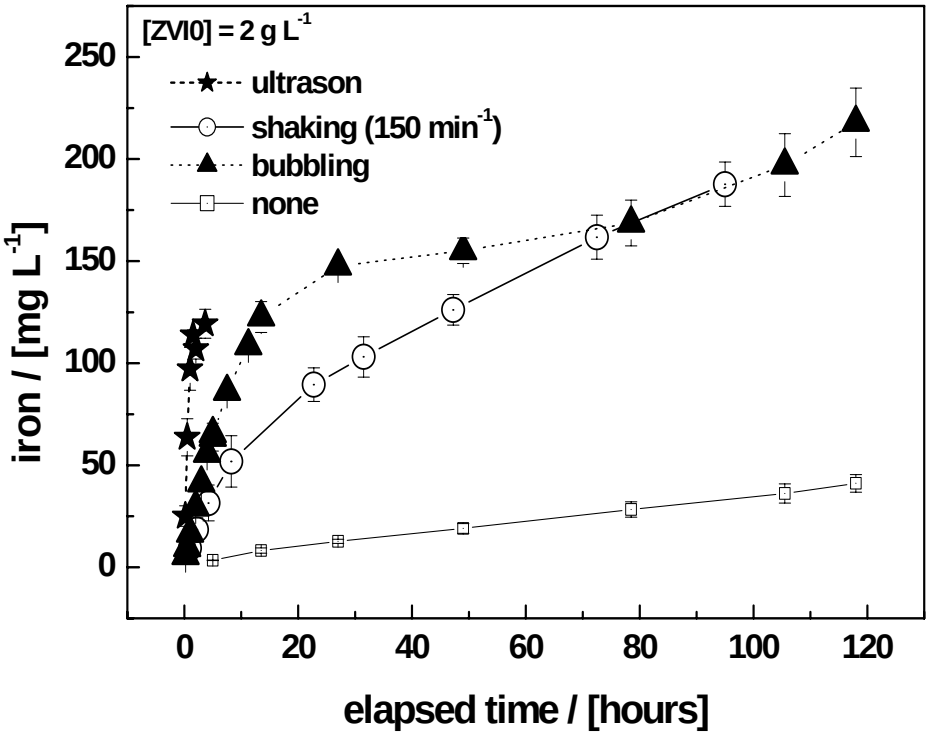

725

726

727

727 **Figure Captions**

728

729 **Figure 1**: Variation of the rate of iron dissolution (k_{EDTA}) as a function of available Fe^0
730 surface for the material ZVI8. The represented lines are not fitting functions, they
731 just joint the points to facilitate visualization.

732

733 **Figure 2**: Effects of the mixing type on the iron dissolution in 0.002 M EDTA. Bubbling and
734 non disturbed experiments were conducted under atmospheric partial pressure of
735 O_2 (open system). Shaking and ultrasound mixing experiments were conducted in
736 closed systems. The represented lines are not fitting functions, they just joint the
737 points to facilitate visualization.

738